Biochemical and Biophysical Research Communications 445 (2014) 89–94

Contents lists available at ScienceDirect

Biochemical and Biophysical Research Communications

journal homepage: www.elsevier.com/locate/ybbrc

Critical function of RA-GEF-2/Rapgef6, a guanine nucleotide exchange factor for Rap1, in mouse spermatogenesis

Keisuke Okada [a], Hideaki Miyake [a], Kohei Yamaguchi [a], Koji Chiba [a], Kazuhiro Maeta [b], Shymaa E. Bilasy [c], Hironori Edamatsu [b], Tohru Kataoka [b,*], Masato Fujisawa [a,*]

[a] Division of Urology, Department of Organs Therapeutics, Kobe University Graduate School of Medicine, 7-5-1 Kusunoki-cho, Chuo-ku, Kobe 650-0017, Japan
[b] Division of Molecular Biology, Department of Biochemistry and Molecular Biology, Kobe University Graduate School of Medicine, 7-5-1 Kusunoki-cho, Chuo-ku, Kobe 650-0017, Japan
[c] Department of Biochemistry, Faculty of Pharmacy, Suez Canal University, El-shikh Zayed, Ismailia 41522, Egypt

ARTICLE INFO

Article history:
Received 20 January 2014
Available online 31 January 2014

Keywords:
RA-GEF-2
Rap1
Small GTPases
Spermatogenesis
Male infertility

ABSTRACT

Small GTPase Rap1 has been implicated in the proper differentiation of testicular germ cells. In the present study, we investigated the functional significance of RA-GEF-2/Rapgef6, a guanine nucleotide exchange factor for Rap1, in testicular differentiation using mice lacking RA-GEF-2. RA-GEF-2 was expressed predominantly on the luminal side of the seminiferous tubules in wild-type mice. No significant differences were observed in the body weights or hormonal parameters of *RA-GEF-2*$^{-/-}$ and wild-type mice. However, the testes of *RA-GEF-2*$^{-/-}$ male mice were significantly smaller than those of wild-type mice and were markedly atrophied as well as hypospermatogenic. The concentration and motility of epididymal sperm were also markedly reduced and frequently had an abnormal shape. The pregnancy rate and number of fetuses were markedly lower in wild-type females after they mated with *RA-GEF-2*$^{-/-}$ males than with wild-type males, which demonstrated the male infertility phenotype of *RA-GEF-2*$^{-/-}$ mice. Furthermore, a significant reduction and alteration were observed in the expression level and cell junctional localization of N-cadherin, respectively, in *RA-GEF-2*$^{-/-}$ testes, which may, at least in part, account for the defects in testicular differentiation and spermatogenesis in these mice.

1. Introduction

Rap1, a member of the Ras superfamily of small GTPases, is involved in regulating a wide variety of cellular functions, including proliferation, differentiation, and cell adhesion [1,2]. To initiate downstream signaling, Rap1 must be converted from an inactive GDP-bound form to an active GTP-bound form that is capable of interacting with various downstream effector molecules [3]. This conversion is greatly facilitated by guanine nucleotide exchange factors (GEFs). To date, a multitude of GEFs for Rap1 have been identified in mammals. Of these, two related GEFs called RA-GEF-1 and RA-GEF-2, also referred to as Rapgef2 and Rapgef6, respectively, constitute an unique Rap1 GEF subfamily [4]. These two GEFs both have GEF and Ras/Rap1-assosiating (RA) domains, which function not only as upstream regulators of Rap1 and Rap2, but also as downstream targets of M-Ras and Rap1. We previously reported that RA-GEF-1, which acts both upstream and downstream of Rap1, facilitated the Rap1-dependent activation of B-Raf in the Golgi apparatus and also that RA-GEF-2 mediated M-Ras-dependent Rap1 activation in the plasma membrane [4].

Rap1 is known to play a critical role in integrin and cadherin-mediated cell adhesion [5–6]. Rap1 was previously shown to be localized at junctions between epithelial and endothelial cells, and was activated at cell–cell contact sites in endothelial cells. Several Rap-specific GEFs, including RA-GEF-2, have also been reported to mediate functions associated with cell–cell adhesion. For example, Dubé et al. demonstrated the crucial role of RA-GEF-2 in the maturation of adherens junctions through the regulation of E-cadherin expression using the lung carcinoma cell line A549 [7]. We also showed that RA-GEF-2 in *RA-GEF-2*$^{-/-}$ mice was responsible for the activation of Rap1, which regulates tumor necrosis factor-α-triggered integrin activation in B lymphocytes [8]. However, associations between RA-GEF-2 and pathological conditions have not yet been examined.

Infertility, defined by the World Health Organization as a period of two years without conception, affects 10–15% of couples, approximately 50% of which has been attributed to male factor

* Corresponding authors. Fax: +81 78 382 5399 (T. Kataoka). Address: Division of Urology, Department of Surgery Related, Faculty of Medicine, Kobe University Graduate School of Medicine, 7-5-1 Kusunoki-Cho, Chuo-Ku, Kobe, 650-0017, Japan. Fax: +81 78 382 6169 (M. Fujisawa).

E-mail addresses: kataoka@people.kobe-u.ac.jp (T. Kataoka), masato@med.kobe-u.ac.jp (M. Fujisawa).

http://dx.doi.org/10.1016/j.bbrc.2014.01.149
0006-291X/

infertility [9]. More than half of infertile men appear to be idiopathic, and, in spite of intensive efforts in the field of male infertility research, effective treatments remain unavailable for these men. However, several studies have recently implicated abnormal cell–cell adhesion in the development of impaired spermatogenesis [10–14]. For example, we previously reported that the disorganized expression of claudin-11, one of the most important tight junction molecules in Sertoli cells, may be one of the factors involved in the impairment of spermatogenesis [13].

Rap1 has recently been implicated in the proper differentiation of testicular germ cells and spermatogenesis [15–20]. We also found that it was very difficult to obtain pups by mating wild-type females with *RA-GEF-2*$^{-/-}$ males. This finding led us to explore the role of RA-GEF-2 in testicular development and spermatogenesis using *RA-GEF-2*$^{-/-}$ males.

2. Materials and methods

2.1. Preparation of *RA-GEF-2*$^{-/-}$ mice

RA-GEF-2$^{-/-}$ mice were generated as described previously [8]. *RA-GEF-2*$^{+/-}$ male mice were crossed with *RA-GEF-2*$^{+/-}$ female mice and the resulting *RA-GEF-2*$^{+/+}$ and *RA-GEF-2*$^{-/-}$ mice were used in the present study at the age of 10–12 weeks. All mice were maintained under standard housing conditions with a 12 to 12-h dark–light cycle at the animal facilities of Kobe University Graduate School of Medicine according to institutional guidelines.

2.2. Quantitative real-time reverse transcription-polymerase chain reaction (qRT-PCR)

qRT-PCR assays were performed as described before [21]. Total RNA was extracted from a testis using TRIzol reagent (Life Technologies Corporation, CA, USA) and reverse transcription to first standard cDNA was performed according to the manufacturer's instructions. RA-GEF-2, N-cadherin, and glyceraldehyde 3-phosphate dehydrogenase (GAPDH) mRNAs were detected using proprietary TaqMan primers and probes (Life Technologies Corporation). The assay identification numbers of the TaqMan probes and primers for RA-GEF-2, N-cadherin, and GAPDH were Mm 01288550 m1, Mm 00561420 m1, and Mm 00667869 m1, respectively. Data on RA-GEF-2 and N-cadherin values were normalized with those of GAPDH values and expressed as arbitrary units relative to the control, set as a value of "1".

2.3. Histology, immunohistochemistry, and immunofluorescence analyses

The testes of age-matched *RA-GEF-2*$^{+/+}$ and *RA-GEF-2*$^{-/-}$ mice were fixed and cut into 4-μm-thick sections after paraffin embedding. Testes samples were de-waxed in xylene and rehydrated through a graded series of ethanol solutions. Sections for histology were stained with hematoxylin and eosin according to standard protocols. Sections for immunohistochemical or immunofluorescence assessments were stained overnight with a primary antibody against mouse RA-GEF-2 (Abnova, Taipei, Taiwan) or rabbit N-cadherin (Santa Cruz Biotechnology, CA, USA), respectively. Slides were washed with phosphate-buffered saline (PBS) and then incubated with an anti-mouse horseradish peroxidase-conjugated antibody (Santa Cruz Biotechnology) or Alexa-Fluor555-conjugated anti-rabbit IgG (Life Technologies Corporation) for 1 h. Sections for immunohistochemistry were then incubated in ABC solution (Vector Laboratories, CA, USA) for 30 min and reacted with metal-3,3-diaminobenzidine (Sigma–Aldrich, MO, USA) for 5 min. Sections for immunofluorescence were mounted on slides with Fluorescence Mounting Medium (Dako, Glostrup, Denmark) and fluorescent images were obtained using a fluorescent microscope (BIOREVO BZ-9000, Keyence, Osaka, Japan).

2.4. Serum collection and biochemical analysis

Blood was collected from each mouse after CO_2 inhalation, incubated at 37 °C for 30 min, and subsequently centrifuged at 3000*g* for 15 min. Serum follicle-stimulating hormone (FSH), luteinizing hormone (LH), and testosterone levels were determined by ELISA assay kits (USCN LIFE SCIENCE, TX, USA) according to the manufacturers' instructions.

2.5. Sperm analysis

Sperm were collected after swimming out from the cauda epididymides into modified Whitten's medium (15 mM Hepes-sodium salt, 1.2 mM $MgCl_2$, 100 mM NaCl, 4.7 mM KCl, 1 mM pyruvic acid, and 4.8 mM lactic acid) for 10 min at 37 °C, with the maintenance of a final pH of 7.35 [22]. Sperm analyses, including the number and motility, were performed using a Makler Counting Chamber (Irvine Scientific, CA, USA). A total of 10 fields were analyzed for each sperm sample.

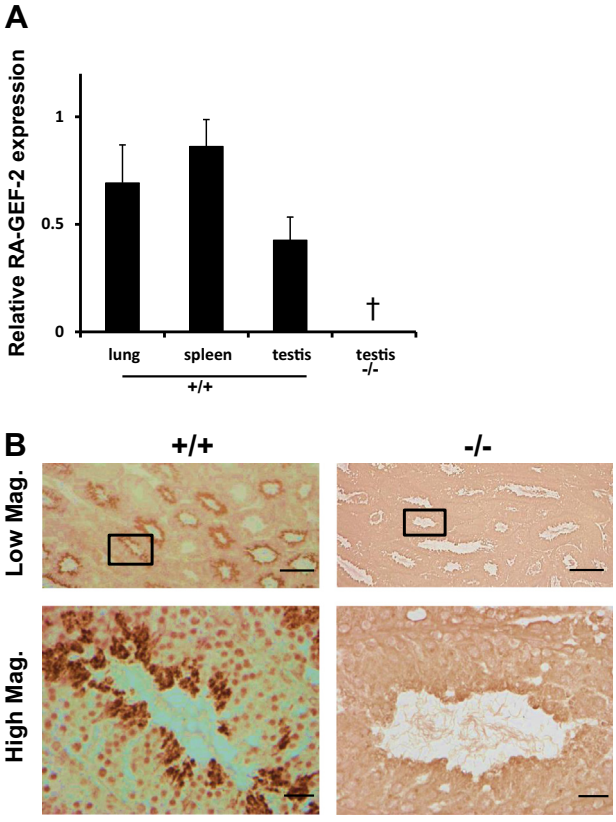

Fig. 1. Expression and localization of RA-GEF-2 in the mouse testis. (A) Total RNA from mice tissue (lung, spleen, or testis) was subjected to quantitative real-time reverse transcription-polymerase chain reaction (qRT-PCR) for the determination of RA-GEF-2 mRNA expression. Columns, mean of the data obtained from 10 *RA-GEF-2*$^{+/+}$ to *RA-GEF-2*$^{-/-}$ mice; bars, SD; † below the detection limit. (B) Immunohistochemical staining of RA-GEF-2 in the testes of *RA-GEF-2*$^{+/+}$ and *RA-GEF-2*$^{-/-}$ mice. The upper and lower panels show low magnitude (Low Mag.) and high magnitude (High Mag.) findings, respectively. The lower panels show enlargements of the boxed areas in the upper panel. Bar = 100 μm (upper panels), 15 μm (lower panels).

2.6. Sperm staining techniques

Semen samples were prepared by placing a 5-μl aliquot onto a slide, smearing using a second slide, followed by air drying for 20–30 s. The Diff-Quick (Medion Diagnostics International, FL, USA) kit was used to stain the smears of semen samples. Diff-Quick fixing and staining times were 5 min and the slides were washed in distilled water to eliminate excess staining, air dried, and covered with a coverslip as previously described [23]. At least 100 sperm per slide were counted to determine the percentage of spermatozoa with abnormal morphologies.

2.7. Scanning electronic microscopy (SEM)

SEM was performed following the standard protocol. Sperm were isolated from the cauda epididymides of mice, allowed to attach to silicon chips, and were then fixed using 4% formaldehyde and 0.1% glutaraldehyde in 2.5 mM $CaCl_2$ in PBS for 30 min [23]. Samples were rinsed 5 times in distilled water for 5 min each and then freeze-dried. The silicon surface with cells was then sputter coated with platinum. Images were obtained using the SEM, JSM-6060 (JEOL, Tokyo, Japan).

2.8. Assessment of fertility and fecundity

To assess fertility and fecundity, each of the littermate males of different genotypes was placed in a cage with two mature wild-type females for at least 2 months. The number of mice achieving a pregnancy and the number of offspring from each pregnancy were recorded.

2.9. Western blot analysis

Western blot analyses were performed as described [24]. Briefly, samples of tissue lysates containing 15 μg of protein were electrophoresed on an SDS–polyacrylamide gel and transferred

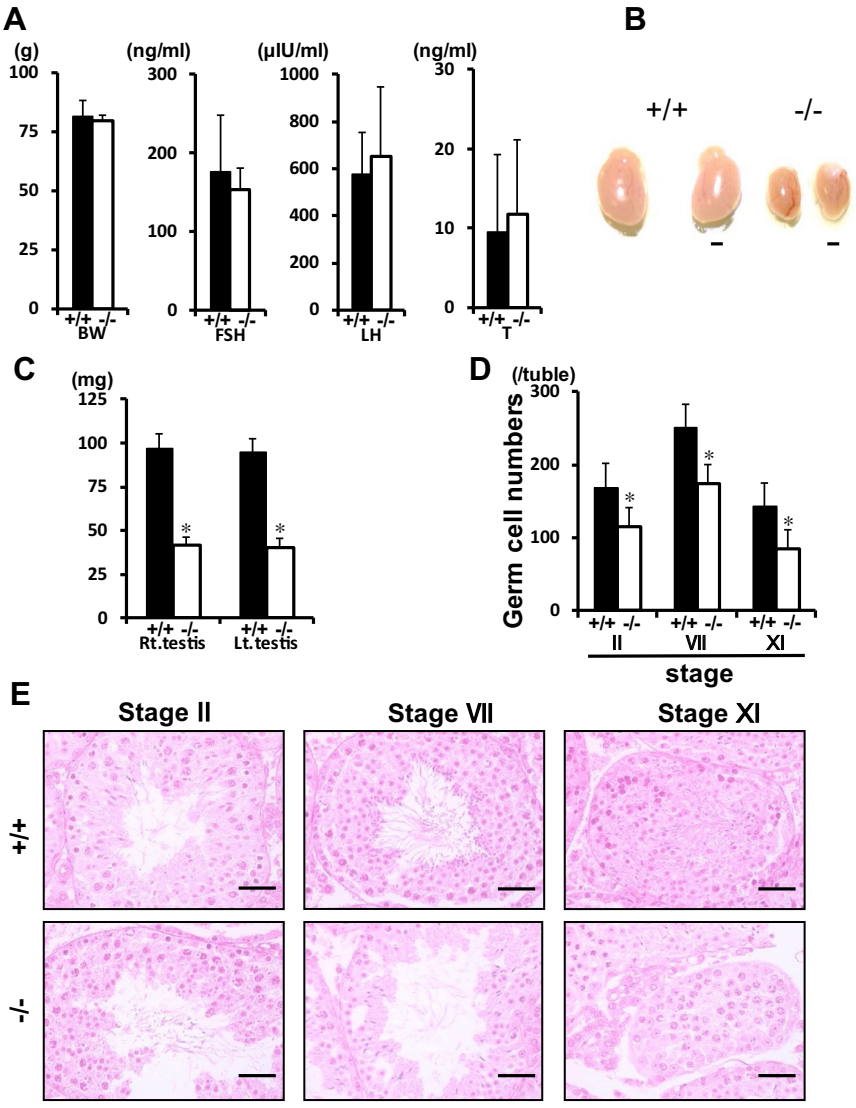

Fig. 2. Abnormalities in the testes of *RA-GEF-2*$^{-/-}$ mice. (A) Body weights and follicle-stimulating hormone (FSH), luteinizing hormone (LH), and testosterone serum levels were compared between *RA-GEF-2*$^{+/+}$ and *RA-GEF-2*$^{-/-}$ mice. Columns, mean of the data obtained from 20 *RA-GEF-2*$^{+/+}$ to *RA-GEF-2*$^{-/-}$ mice; bars, SD. (B) Macroscopic appearance of the testes of *RA-GEF-2*$^{+/+}$ and *RA-GEF-2*$^{-/-}$ mice. Bar = 1 mm. (C) Testis weights were compared between *RA-GEF-2*$^{+/+}$ and *RA-GEF-2*$^{-/-}$ mice. Columns, mean of the data from 20 *RA-GEF-2*$^{+/+}$ to *RA-GEF-2*$^{-/-}$ mice; bars, SD. ∗ differs from the value of *RA-GEF-2*$^{+/+}$ mice ($P < 0.01$). (D) Germ cell numbers per seminiferous tubule were compared at different stages (stage II, VII, and XI) of mouse spermatogenesis between *RA-GEF-2*$^{+/+}$ and *RA-GEF-2*$^{-/-}$ mice. Columns, mean of the data obtained from 20 *RA-GEF-2*$^{+/+}$ to *RA-GEF-2*$^{-/-}$ mice; bars, SD. ∗ differs from the value of *RA-GEF-2*$^{+/+}$ mice ($P < 0.01$). (E) Histological findings of testis sections from *RA-GEF-2*$^{+/+}$ to *RA-GEF-2*$^{-/-}$ mice stained with Hematoxylin–Eosin at different stages (stage II, VII, and XI) of mouse spermatogenesis. Bar = 20 μm.

to a nitrocellulose filter. The filters were blocked in PBS containing 5% non-fat milk powder at 4 °C overnight and then incubated for 1 h with an antibody against N-cadherin or β-actin (Sigma–Aldrich). The filters were incubated for 30 min with horseradish peroxidase-conjugated secondary antibodies and specific proteins were then detected using an enhanced chemiluminescence Western blotting system (GE Healthcare UK Ltd, Buckinghamshire, England).

2.10. Statistical analysis

All data are presented as mean values ± standard deviations (SDs) unless otherwise stated. The statistical evaluation of means between two data sets was performed using the Student's *t*-test. *P* values <0.05 were considered significant.

3. Results

3.1. Expression and localization of RA-GEF-2 in the testis

The relative expression levels of RA-GEF-2 in several organs including the testes of *RA-GEF-2*$^{+/+}$ and *RA-GEF-2*$^{-/-}$ mice were analyzed using qRT-PCR, which showed that RA-GEF-2 was expressed in the testes of *RA-GEF-2*$^{+/+}$, but not *RA-GEF-2*$^{-/-}$ mice (Fig. 1A). Immunohistochemical staining detected RA-GEF-2 predominantly on the luminal side of the seminiferous tubules (Fig. 1B).

3.2. Abnormalities in the testes of RA-GEF-2$^{-/-}$ mice

RA-GEF-2$^{-/-}$mice grew normally and their body weights and FSH, LH, and testosterone serum levels were not significant different from those of *RA-GEF-2*$^{+/+}$ mice (Fig. 2A). Anatomical examinations revealed that the spleens of *RA-GEF-2*$^{-/-}$ mice were larger than those of *RA-GEF-2*$^{+/+}$ mice, which has been reported previously [6]. In addition, the testes of *RA-GEF-2*$^{-/-}$ mice were significantly smaller than those of *RA-GEF-2*$^{+/+}$ mice (Fig. 2B and C).

Fig. 2E shows a histological comparison of the seminiferous epithelial cycle according to the stage between *RA-GEF2*$^{+/+}$ and *RA-GEF-2*$^{-/-}$ mice. Hematoxylin–Eosin staining revealed marked atrophy of the testes and enlargement of the lumens in the seminiferous tubules of *RA-GEF-2*$^{-/-}$, but not *RA-GEF2*$^{+/+}$ mice throughout the stages examined. Moreover, severe hypospermatogenesis was observed in *RA-GEF-2*$^{-/-}$ mice, as shown by quantitative measurements of germ cell numbers at each stage (Fig. 2D and E).

3.3. Characterization of sperm and assessment of fertility in RA-GEF-2$^{-/-}$ mice

The epididymal sperm concentration of *RA-GEF-2*$^{-/-}$ mice was markedly lower than that of *RA-GEF-2*$^{+/+}$ mice. The sperm motility and normal morphology rates were also lower in *RA-GEF-2*$^{-/-}$ mice (Fig. 3A). Sperm morphology was examined both by light microscopy of smears and SEM. As shown in Fig. 3B, a representative sperm from *RA-GEF-2*$^{-/-}$ mice had a rounder shaped head than that from *RA-GEF-2*$^{+/+}$ mice with a normal morphology.

When presented with wild-type female mice in mating cages, both *RA-GEF-2*$^{+/+}$ and *RA-GEF-2*$^{-/-}$ male mice exhibited normal libidos; evidence of ejaculation in the form of vaginal plugs was commonly found in all female mice within a few days. However, the successful mating rates and number of fetuses were significantly lower when females were mated with *RA-GEF-2*$^{-/-}$ male mice (Fig. 3C).

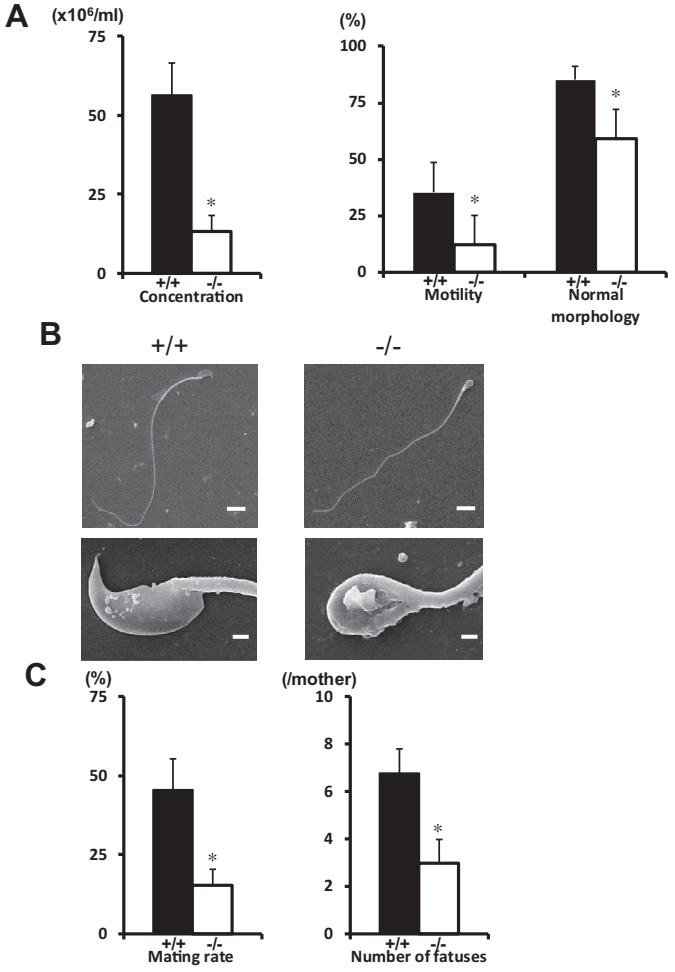

Fig. 3. Characterization of sperm and assessment of fertility in *RA-GEF-2*$^{-/-}$ mice. (A) Sperm concentrations and sperm motility and normal morphology rates were compared between *RA-GEF-2*$^{+/+}$ and *RA-GEF-2*$^{-/-}$ mice. Columns, mean of the data obtained from 20 *RA-GEF-2*$^{+/+}$ to *RA-GEF-2*$^{-/-}$ mice; bars, SD. ∗ differs from the value of *RA-GEF-2*$^{+/+}$ mice ($P < 0.01$). (B) Morphological findings on sperm from *RA-GEF-2*$^{+/+}$ to *RA-GEF-2*$^{-/-}$ mice visualized using scanning electron micrographs. Bar = 10 μm (upper panels), 1 μm (lower panels). (C) After mating with wild type female mice, successful mating rates and the average number of fetuses between *RA-GEF-2*$^{+/+}$ and *RA-GEF-2*$^{-/-}$ mice were compared. Columns, mean of the data obtained from 11 *RA-GEF-2*$^{+/+}$ to 13 *RA-GEF-2*$^{-/-}$ mice; bars, SD. ∗ differs from the value of *RA-GEF-2*$^{+/+}$ mice ($P < 0.01$).

3.4. Altered expression and localization of N-cadherin in the testes of RA-GEF-2$^{-/-}$ mice

Considering the previously clarified function of the GEFs-Rap1 axis [4–6] and localization of RA-GEF-2 in the testis (Fig. 1B), the expression patterns of molecules associated with the formation of adherens junctions, including E-cadherin, N-cadherin, nectins, and integrins [25,26], were investigated. As shown in Fig. 4A and B, the expression level of N-cadherin in the testes of *RA-GEF-2*$^{-/-}$ mice was significantly lower than that in *RA-GEF-2*$^{+/+}$ mice at both the mRNA and protein levels. In contrast, no significant difference was observed in the expression levels of the remaining molecules examined in this study (data not shown). Immunofluorescence analysis showed that N-cadherin was condensed at certain cellular junctions that were arranged in a radial fashion in the seminiferous tubules of *RA-GEF-2*$^{+/+}$ mice. This radial localization pattern became irregular and diffuse in *RA-GEF-2*$^{-/-}$ mice (Fig. 4C).

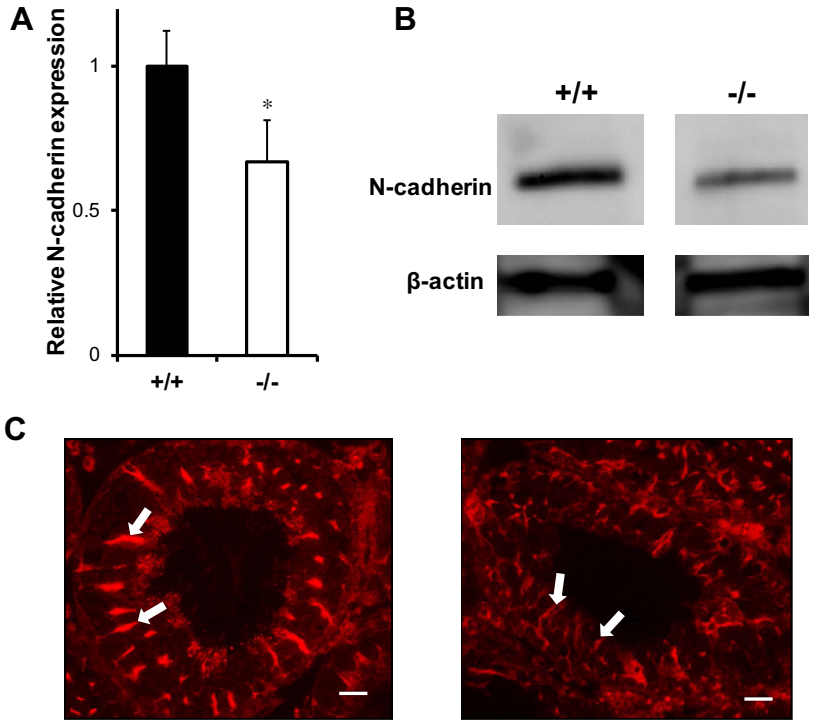

Fig. 4. Expression and localization of N-cadherin in the testes of *RA-GEF-2*$^{-/-}$ mice (A) Relative mRNA expression levels of N-cadherin in the testes of *RA-GEF-2*$^{+/+}$ and *RA-GEF-2*$^{-/-}$ mice evaluated by quantitative real-time reverse transcription-polymerase chain reaction (qRT-PCR) assays. Columns, mean of the data obtained from 10 *RA-GEF-2*$^{+/+}$ and *RA-GEF-2*$^{-/-}$ mice; bars, SD. ∗ differs from the value of *RA-GEF-2*$^{+/+}$ mice ($P < 0.01$). (B) Expression of N-cadherin in the testes of *RA-GEF-2*$^{+/+}$ and *RA-GEF-2*$^{-/-}$ mice evaluated by Western blotting. (C) Immunofluorescence staining for N-cadherin in the testes of *RA-GEF-2*$^{+/+}$ and *RA-GEF-2*$^{-/-}$ mice. White arrows show the expression of N-cadherin.

4. Discussion

Several recent studies have shown the involvement of Rap1 in mammalian spermatogenesis [15–20]. For example, Yang et al. reported that the most intensive accumulation of Rap1 protein during spermatogenesis occurred in the pachytene spermatocytes of adults and also that Rap1 may play an important role in the early stage of the apoptotic process in the rat testis induced by methoxyacetic acid, which selectively depletes primary spermatocytes, in cooperation with NF-κB [15,16]. In addition, Aivatiadou et al. generated transgenic mice selectively expressing an inactive Rap1 mutant in differentiating spermatids and showed that interfering with Rap1 function during spermiogenesis led to reduced fertility through an impairment in germ-Sertoli cell contacts [17]. However, no study has yet explored the significance of GEFs, upstream activators of Rap1, in spermatogenesis. Thus, we investigated the functional role of RA-GEF-2 in the process of spermatogenesis using *RA-GEF-2*$^{-/-}$ mice.

RA-GEF-1 was previously shown to be ubiquitously expressed in mouse tissues, and the expression level of RA-GEF-2 was particularly high in the spleen and thymus, but was weak or undetectable in other tissues [8]. In this study, we initially confirmed the expression of RA-GEF-2 in the testes, which was localized on the luminal side of seminiferous tubules. Moreover, in spite of the lack of significant differences in body weights and hormonal parameters, *RA-GEF-2*$^{-/-}$ mice had markedly smaller testes, accompanied by severe hypospermatogenesis, than those of *RA-GEF-2*$^{+/+}$ mice. These results strongly indicated the important function of RA-GEF-2 in the development of the testes and maintenance of normal spermatogenesis.

We then investigated the effects of a RA-GEF-2 deficiency on the characteristics of sperm and found that both the concentration and motility of sperm in *RA-GEF-2*$^{-/-}$ mice were significantly lower than those in *RA-GEF-2*$^{+/+}$ mice and also that malformed sperm were ubiquitously observed in *RA-GEF-2*$^{-/-}$ mice. In addition, successful mating rates with wild-type female mice were significantly lower in RA-GEF-2$^{-/-}$ mice in spite of normal libidos. Considering these results, the pathological conditions associated with spermatogenesis and fertility observed in *RA-GEF-2*$^{-/-}$ mice appeared to be similar to those observed in oligoasthenoteratozoospermia (OAT) syndrome, which is characterized by the simultaneous occurrence of oligozoospermia, asthenozoospermia, and teratozoospermia and is recognized as the most frequently observed condition in men diagnosed with idiopathic male infertility. Therefore, we believe that *RA-GEF-2*$^{-/-}$ mice could serve as an useful animal model for investigating the molecular mechanisms underlying OAT syndrome.

Spermatogenesis is at least in part, dependent on the ability of Sertoli cells to form mature junctions that maintain an unique environment within the seminiferous epithelium. Several previous studies have reported an association between a disorder in the adherence junction and impaired spermatogenesis. Therefore, we focused on changes in molecules that mediated the formation of the adherence junction in an attempt to elucidate the mechanism underlying hypospermatogenesis of *RA-GEF-2*$^{-/-}$ mice. Of the several molecules examined in this study, N-cadherin expression in the testes was significantly reduced in *RA-GEF-2*$^{-/-}$ mice. Moreover, the radial localization of N-cadherin in the seminiferous tubules, which may correspond to the adherence junction between Sertoli cells and germ cells, was compromised in *RA-GEF-2*$^{-/-}$ mice. N-cadherin, which was initially identified as a cell adhesion molecule expressed in neural tissues [27], was mainly distributed in the junctional complex formed by adjacent Sertoli cells including classical adherence junctions and testis-specific ectoplasmic specializations [28–31]. Collectively, these findings suggest that RA-GEF-2 may be involved in the formation of the mature

junctional complex between Sertoli cells and germ cells to maintain normal spermatogenesis through the regulation of N-cadherin expression and localization.

There were several limitations to this study. The localization patterns of RA-GEF-2 as well as N-cadherin should be more precisely investigated in mouse testes to clarify the functional role of these proteins during spermatogenesis. In addition, the impact of the signal transduction pathway via the GEFs-Rap1 axis, rather than that using RA-GEF-2-deficient mice alone, on spermatogenesis should be more comprehensively characterized. Finally, we need to determine whether the current results obtained in a mouse model can be applied to pathophysiological conditions in humans.

In conclusion, we confirmed the expression of RA-GEF-2 in the mouse testis, and demonstrated that the loss of RA-GEF-2 resulted in severe hypospermatogenesis, which was accompanied by a significant decrease in the concentration and motility of sperm as well as ubiquitous sperm malformation. Furthermore, successful mating rates with wild type female mice were shown to be significantly lower in the RA-GEF-2-deficient mice. N-cadherin appeared to be down-regulated and diffusely expressed in RA-GEF-2-deficient mice. Taken together, these results suggest that RA-GEF-2 may play an important role in the maintenance of spermatogenesis and also that the RA-GEF-2-deficient mice used in this study could represent an attractive model for investigating spermatogenesis disorders, such as OAT syndrome.

Acknowledgments

We thank Dr. Tatsuya Nagano (Kobe University, Kobe, Japan) for valuable discussions. We thank Emmy Yanagita (Kobe University Hospital, Kobe, Japan) for her thoughtful and helpful advice regarding immunohistochemistry.

References

[1] J.L. Bos, Linking Rap to cell adhesion, Curr. Opin. Cell Biol. 17 (2005) 123–128.
[2] M. Duchniewicz, T. Zemojtel, M. Kolanczyk, S. Grossmann, J.S. Scheele, F.J. Zwartkruis, Rap1A-deficient T and B cells show impaired integrin-mediated cell adhesion, Mol. Cell. Biol. 26 (2006) 643–653.
[3] L.A. Quilliam, J.F. Rebhun, A.F. Castro, A growing family of guanine nucleotide exchange factors is responsible for activation of Ras-family GTPases, Prog. Nucleic Acid Res. Mol. Biol. 71 (2002) 391–444.
[4] X. Gao, T. Satoh, Y. Liao, C. Song, C.D. Hu, T. Kataoka, et al., Identification and characterization of RA-GEF-2, a Rap guanine nucleotide exchange factor that serves as a downstream target of M-Ras, J. Biol. Chem. 45 (2001) 42219–42225.
[5] K.A. Reedquist, E. Ross, E.A. Koop, R.M. Wolthuis, F.J. Zwartkruis, Y. van Kooyk, et al., The small GTPase, Rap1, mediates CD31-induced integrin adhesion, J. Cell Biol. 6 (2000) 1151–1158.
[6] M.R. Kooistra, N. Dubé, J.L. Bos, Rap1: a key regulator in cell–cell junction formation, J. Cell Sci. 120 (2007) 17–22.
[7] N. Dubé, M.R. Kooistra, W.J. Pannekoek, M.J. Vliem, V. Oorschot, J. Klumperman, et al., The RapGEF PDZ-GEF2 is required for maturation of cell–cell junctions, Cell Signal. 9 (2008) 1608–1615.
[8] Y. Yoshikawa, T. Satoh, S.E. Bilasy, H. Edamatsu, T. Kataoka, et al., The M-Ras-RA-GEF-2-Rap1 pathway mediates tumor necrosis factor-alpha dependent regulation of integrin activation in splenocytes, Mol. Biol. Cell 18 (2007) 2949–2959.
[9] J. Poongothai, T.S. Gopenath, S. Manonayaki, Genetics of human male infertility, Singapore Med. J. 4 (2009) 336–347.
[10] N.P. Lee, C.Y. Cheng, Ectoplasmic specialization, a testis-specific cell-cell actin-based adherens junction type: is this a potential target for male contraceptive development, Hum. Reprod. Update 10 (2004) 349–369.
[11] H.H. Yan, D.D. Mruk, C.Y. Cheng, Junction restructuring and spermatogenesis: the biology, regulation, and implication in male contraceptive development, Curr. Top. Dev. Biol. 80 (2008) 57–92.
[12] C.Y. Cheng, E.W. Wong, P.P. Lie, D.D. Mruk, X. Xiao, et al., Polarity proteins and actin regulatory proteins are unlikely partners that regulate cell adhesion in the seminiferous epithelium during spermatogenesis, Histol. Histopathol. 26 (2011) 1465–1474.
[13] K Chiba, K Yamaguchi, M Ando, H Miyake, M. Fujisawa, Expression pattern of testicular claudin-11 in infertile men, Urology 80 (5) (2012) 1161.e13-7.
[14] X. Xiao, D.D. Mruk, C.Y. Cheng, Polarity proteins and actin regulatory proteins are unlikely partners that regulate cell adhesion in the seminiferous epithelium during spermatogenesis, Hum. Reprod. Update 19 (2013) 167–186.
[15] B. Yang, H. Wang, X.K. Gao, B.Q. Chen, Y.Q. Zhang, H.L. Liu, et al., Expression and significance of Rap1A in testes of azoospermic subjects, Asian J. Androl. 6 (2004) 35–40.
[16] B. Yang, H. Sun, W. Li, C. Zhu, B. Jian, W. Hou, et al., Expression of Rap1 during germ cell development in the rat and its functional implications in 2-methoxyacetic acid-induced spermatocyte apoptosis, Urology 81 (2013) 696.e1-8.
[17] E. Aivatiadou, E. Mattei, M. Ceriani, L. Tilia, G. Berruti, Impaired fertility and spermiogenetic disorders with loss of cell adhesion in male mice expressing an interfering Rap1 mutant, Mol. Biol. Cell 18 (2007) 1530–1542.
[18] E. Aivatiadou, M. Ripolone, F. Brunetti, G. Berruti, CAMP-Epac2-mediated activation of Rap1 in developing male germ cells: RA-RhoGAP as a possible direct down-stream effector, Mol. Reprod. Dev. 76 (2009) 407–416.
[19] H. Scherthan, A. Sfeir, T. de Lange, Rap1-independent telomere attachment and bouquet formation in mammalian meiosis, Chromosoma 120 (2011) 151–157.
[20] E.A. Ahmed, A. Sfeir, H. Takai, H. Scherthan, Ku70 and non-homologous end joining protect testicular cells from DNA damage, J. Cell Sci. 126 (2013) 3095–3104.
[21] K. Yamaguchi, T. Ishikawa, Y. Kondo, M. Fujisawa, Cisplatin regulates Sertoli cell expression of transferrin and interleukins, Mol. Cell. Endocrinol. 283 (2008) 68–75.
[22] Z. Zhang, I. Kostetskii, W. Tang, L. Haig-Ladewig, R. Sapiro, Z. Wei, et al., Deficiency of SPAG16L causes male infertility associated with impaired sperm motility, Biol. Reprod. 74 (2006) 751–759.
[23] V. Selvaraj, A. Asano, D.E. Buttke, J.L. McElwee, J.L. Nelson, C.A. Wolff, et al., Segregation of micron-scale membrane sub-domains in live murine sperm, J. Cell Physiol. 206 (2006) 636–646.
[24] K. Chiba, Y. Kondo, K. Yamaguchi, H. Miyake, M. Fujisawa, Inhibition of claudin-11 and occludin expression in rat Sertoli cells by mono-(2-ethylhexyl) phthalate through p44/42 mitogen-activated protein kinase pathway, J. Androl. 33 (2012) 368–374.
[25] I.A. Kopera, B. Bilinska, C.Y. Cheng, D.D. Mruk, Sertoli-germ cell junctions in the testis: a review of recent data, Philos. Trans. R. Soc. London B Biol. Sci. 27 (2010) 1593–1605.
[26] Y. Takai, W. Ikeda, H. Ogita, Y. Rikitake, The immunoglobulin-like cell adhesion molecule nectin and its associated protein afadin, Annu. Rev. Cell Dev. Biol. 24 (2008) 309–342.
[27] M. Takeichi, The cadherins: cell–cell adhesion molecules controlling animal morphogenesis, Development 102 (1988) 639–655.
[28] A.M. Andersson, K. Edvardsen, N.E. Skakkebaek, Expression and localization of N- and E-cadherin in the human testis and epididymis, Int. J. Androl. 17 (1994) 174–180.
[29] D.Y. Zhang, D.W. He, G.H. Wei, X. Liu, T. Lin, X.L. Li, Phyllanthus urinaria extract promotes N-cadherin expression in nitrogen mustard-disrupted testicular tissues in vivo, Zhonghua Nan Ke Xue 14 (2008) 396–400.
[30] K.J. Johnson, K. Boekelheide, Dynamic testicular adhesion junctions are immunologically unique. II. Localization of classic cadherins in rat testis, Biol. Reprod. 66 (2002) 992–1000.
[31] C.Y. Cheng, D.D. Mruk, Cell junction dynamics in the testis: Sertoli–germ cell interactions and male contraceptive development, Physiol. Rev. 82 (2002) 825–874.